Ahmed H. Abood [1]
Asmiet Ramizy [1]
Borhan A. Albiss [2]

[1] *Department of Physics, College of Science, University of Anbar, Anbar, IRAQ*
[2] *Department of Physics, College of Science, Jordan University of Science & Technology, Irbid, JORDAN*

Photoresponsive Analysis of Zinc Telluride Broadband Photodetector Fabricated using Pulsed Laser Deposition Technique

In this work, zinc telluride (ZnTe) films were deposited on n-type silicon and FTO glass substrate by using the pulsed laser deposition technique at an energy of 180 mJ with various numbers of pulses (900 and 700). X-ray diffraction results revealed that the synthesised ZnTe nanostructures have a polycrystalline, cubic structure in a crystallisation direction (111) and high intensity, with the absence of the hexagonal phase. FE-SEM revealed that all the films are homogeneous and free of voids and cracks. The energy gap decreased from 2.86 eV to 2.74 eV when the number of laser pulses increased. Silver (Ag) electrodes were deposited on the films, and detection tests were conducted. The spectral response of the detector increased from 15.706 μA/mW to 27.028 μA/mW when the number of pulses increased from 700 to 900. The specific detectivity and quantum efficiency increased from 7.92 ×10^{17} Jones to 8.54 ×10^{17} Jones and from 42.338% to 72.85%, respectively, when the number of pulses increased. The response and recovery times were 0.31 and 0.34 s, respectively.

Keywords: Heterojunctions; Pulsed-laser deposition; Recovery time; Quantum efficiency
Received: 26 April 2024; Revised: 14 July 2024; Accepted: 21 July 2024

1. Introduction

To date, visible-light photodetector, through which incident spectrum can be distinguished via the conversion of optical signal into electrical information, is extensively investigated owing to its wide-reaching applications in optical communications, space-based research and environmental monitoring [1-4]. Assembly II–IV compound semiconductors including cadmium selenide (CdSe), zinc selenide (ZnSe), zinc telluride (ZnTe) and cadmium telluride (CdTe) have elicited remarkable attention owing to their low cost and high absorption coefficients in their applications in a variety of solid-state devices [4]. ZnTe has received great attention from researchers due to its low cost and high absorption coefficient. Therefore, it can be used in photovoltaic applications in the visible region, such as solar cells and photodetectors [5]. ZnTe is a chemical compound in the form of a grey or reddish-brown powder. ZnTe is polycrystalline with a zinc-blended cubic crystal structure, is usually of the p-type, has an energy gap of 1.7–2.4 eV at room temperature and is broadly used in modern optoelectronic technologies [6,7]. ZnTe can also be prepared in the form of hexagonal crystals with a fixed lattice of 0.6101 nm. ZnTe has an electronic affinity of 3.5 eV [8]. ZnTe thin films are generally used in fabricating different solid-state optoelectronic devices (solar cells, photodetectors, light emitting diodes and laser diodes) due to their electrical properties and specific optical properties (high transparency in infrared and visible regions and low electrical resistivity) [9,10].

Heterojunctions are important in semiconductor devices such as photo detector, solar cells, light-emitting diode and integrated circuits [11,12]. A heterojunction is a junction formed between two dissimilar semiconductors and can be classified into two types, namely, graded and abrupt, according to the distances during which the transition from one material to the other is completed near the interface. Another classification is according to the type of the conductivity present on either side of the junction. An isotype heterojunction (p–p) or (n–n) is formed when two semiconductors have the same type of conduction, whereas an isotype heterojunction (p–n) or (n–p) is formed when the conductivity type differs. The pulse laser deposition (PLD) technique is suitable for growing films with high quality at low temperatures [13,14]. The PLD technique involves three main steps: ablation of the target material, high-energy column formation and film growth on the substrate. A high-power laser is used as the energy source to vaporise a target containing the desired film components.

In this work, a photodetector device was synthesised using a thin film with ZnTe/Si heterostructure through PLD, and the characteristics of the fabricated device were studied.

2. Experimental Part

ZnTe powder with a purity of 99.99 was used. The powder was pressed by a hydraulic press to make the target in the form of a disk with a thickness of 0.5 cm and a diameter of 2 cm. Next, ZnTe films were deposited on a Si (111) substrate (n-type). Using the PLD technique, the substrate was placed parallel to the target to obtain good, homogeneous films. The deposition was performed inside a vacuum chamber evacuated to a pressure of 4×10^{-4} mbar by using an

 © ALL RIGHTS RESERVED

Nd:YAG laser with a wavelength of 1064 nm, a frequency of 6 Hz, and an energy of 180 mJ at 700 and 900 pulses. Photodetectors were fabricated by deposition silver metal (Ag) on ZnTe/Si using a metal mask containing a set of surface holes using the thermal evaporation method under high-vacuum 10^{-4} mbar. Detection tests were conducted, which included (current–voltage) characteristics in illuminated and dark, spectral response, detectivity and external quantum efficiency.

3. Results and discussion

Figure (1) shows the XRD pattern of ZnTe films prepared at 700 and 900 pulses. The films have polycrystalline, cubic structures with different crystallographic directions, which are (111), (220), (440) and (331). Comparing the peaks and their intensities finds that the dominant phase of growth is the direction of (111); this result agrees with other studies [15, 16]. These results are consistent with the card (JCPDS Number 15-0746) for ZnTe. The other peaks are (102), (200), (211) and (220) from the FTO substrate, according to the card (JCPDS Number 041-1445). The high intensity of any peak can be explained by the fact that most of the crystals formed have the same orientation (hkl) and reflect all the X-rays incident in the same direction. Therefore, the crystal size increases as the intensity of the rays increases and as the FWHM value decreases. The value of FWHM for all peaks decreases with the increase in the number of laser pulses (increasing the thickness of the film). This outcome indicates a decrease in crystalline defects due to the increase in crystalline size; the rate of crystalline size increases when the number of laser pulses increases due to the rapid growth of the crystallisation; thus, the crystalline defects of the films prepared are removed, this behaviour has been observed in other studies [16].

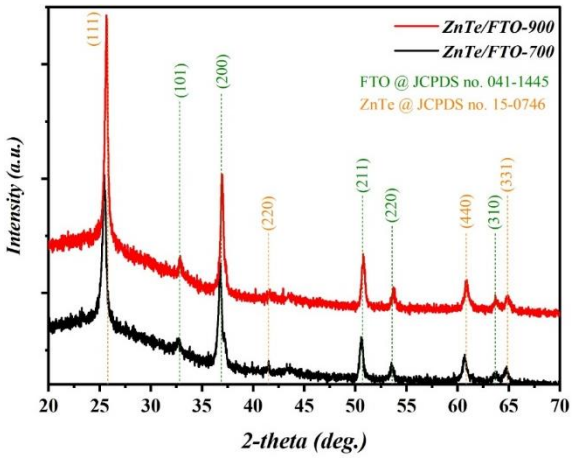

Fig. (1) XRD patterns for ZnTe/FTO at different laser pulses (700 and 900) pulses

Figure (2) shows FE-SEM images of ZnTe/Si films prepared at an energy of 180 mJ and different numbers of laser pulses (700 and 900). All films have homogeneous, smooth surfaces, full and dense with cohesive grains, and free of holes and cracks, which indicates that all films have a good adhesion to substrate surfaces without mismatching. When the number of laser pulses increases, particles of different sizes appear on the surface of the films; their number and size increase with the increase in the number of laser pulses. The reason for this is the agglomeration of the particles with one another to produce larger particles [17]. The average particle diameter increases from 20.35 nm to 22.61 nm with an increase in the number of laser pulses from 700 to 900.

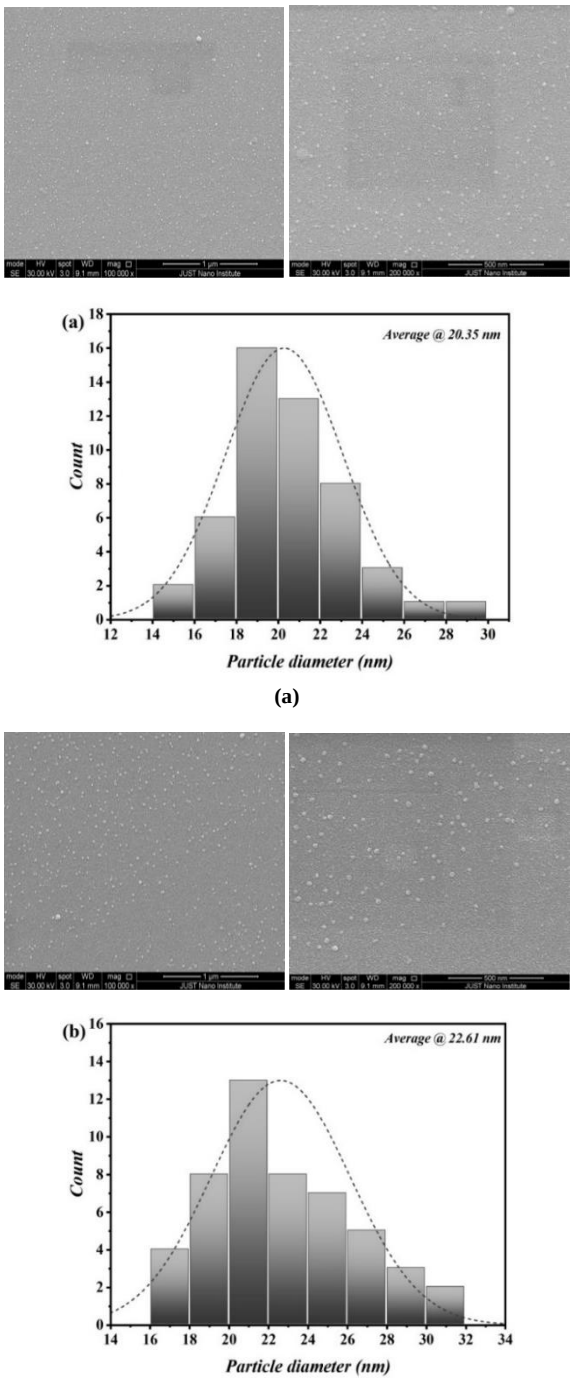

Fig. (2) FE-SEM images of ZnTe/Si prepared using (a) 700 and (b) 900 pulses at 180 mJ

 © ALL RIGHTS RESERVED

Figure (3) shows the energy-dispersive X-ray (EDX) spectrum to confirm the chemical composition of the ZnTe/Si nanostructure. The strong peaks in the spectrum are related to zinc, tellurium, oxygen and silicon from the substrate. The EDX analysis of ZnTe nanostructure films reveals that zinc, tellurium and oxygen are the only main detected elements in the films, and this indicates the good purity of the prepared films.

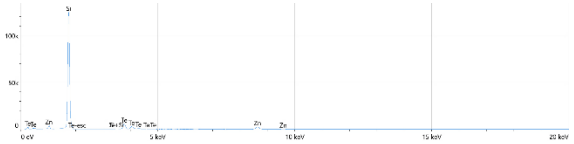

Element	Weight %
O	4.4
Si	72.1
Zn	6.9
Te	16.6

Fig. (3) EDX spectrum of ZnTe synthesized using 700 laser pulses at 180 mJ

Figure (4) presents the energy gap values for ZnTe/Si films prepared at (180 mj, 700 and 900 pulses). The energy gap value for the ZnTe film decreases from 2.7 eV to 2.62 eV when the number of laser pulses increases from 700 to 900; such outcomes are close to the results obtained by others [18]; the bandgap was estimated using Tauc relation [19]. This decrease in the energy gap values could be due to the increase in the thickness of the film when the number of laser pulses increases; thus, the atoms become close together, leading to the formation of energy levels that overlap with the energy gap of these films. Consequently, the energy bands expand, and the optical energy gap of the prepared films decreases. A possible reason is that the removal of some local levels present in the optical energy gap leads to a decrease in its value [20].

Figure (5) exhibits the behaviour of the dark and illuminated currents as a function of the forward and reverse bias voltages for a ZnTe/Si detector fabricated for different light intensities (6, 14 and 26 mW/cm^2). The results for the dark current show that at low voltages (V<1 Volts), the current exponentially rises with the increase of the applied voltage and the recombination current dominates, whereas at high voltages (V>1 Volts), the diffusion current dominates [21]. When a light is shined on the detector, the photocurrent increases with the increase of the bias voltage because the height of the depletion region increases with increase of the applied bias voltage due to the separation of the e–h pairs and then increases the photocurrent [22]. When incident power density increases, the response of all fabrication detectors increases, and that through increased illumination current values with increased incident power density. This outcome is due to the increasing intensity of incident light, where an increase in the number of incident photons leads to an increase in the number of generated charge carriers, which spread within the depletion region and then increase the generated illumination current with increasing incident power density [23].

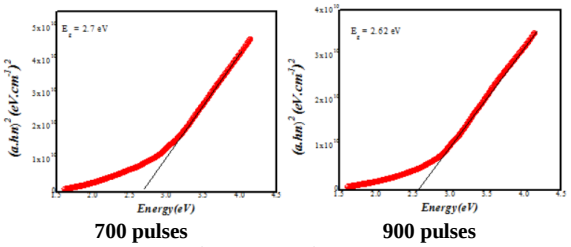

700 pulses 900 pulses

Fig. (4) Energy gap of ZnTe thin film prepared using 700 and 900 laser pulses

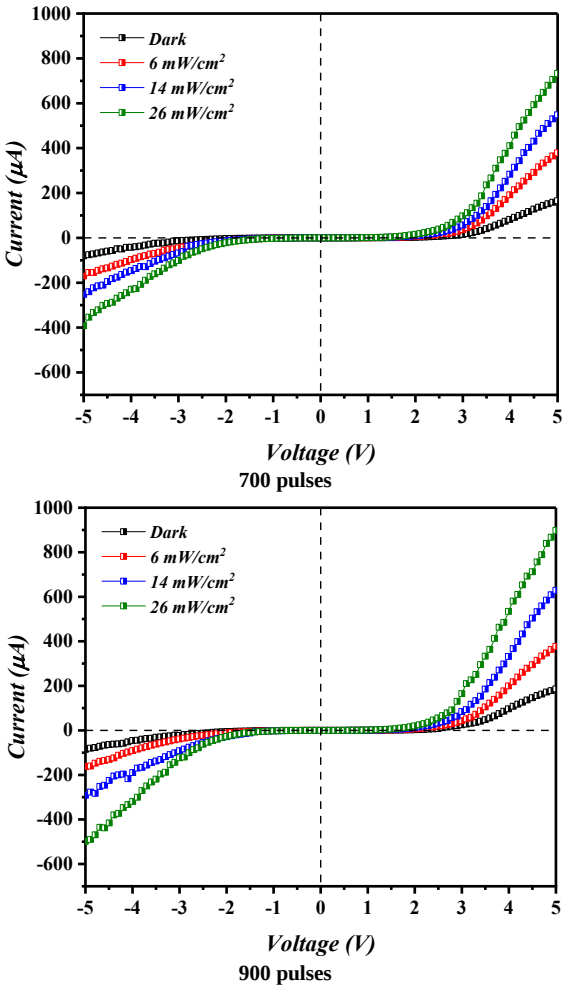

Fig. (5) I-V characteristics of ZnTe/Si photodetectors prepared at different number of laser pulses at laser energy 180 mJ

Figure (6) shows on/off measurements are performed to verify the response/recovery time and the switching behaviour of the fabricated photodetectors. The photoelectric current of the detector, fabricated at 700 pulses, reaches its maximum at a response time of 0.31 s and then decreases to its initial amount (dark current) at a recovery time of 0.34 s. This outcome indicates the

 © ALL RIGHTS RESERVED

rapid injection of electrons and the slow recombination of excited electrons [12].

The response time of the fabricated detector at 900 pulses is 0.34 s, and the recovery time is 0.32 s. The fabricated detector achieves a stable performance for three consecutive cycles, which indicates the satisfactory consistency of the detector. This result shows the good switching property and the durability of the ZnTe/Si detector fabricated at (900) pulses.

Spectral responsivity is an important parameter for detectors and can be calculated through the following equation:

$$R_\lambda = \frac{I_{ph}(A)}{P_\lambda(W)}, \quad [24, 25]$$

where I_{ph} is the photo current, and P_λ is the light power.

Figure (7) illustrates the spectral responsivity curves as a function of wavelength for ZnTe/Si detectors fabricated at different laser pulses. The spectrum of responsivity is related to the spectral character of the density of states, which is reflected by the photocurrent. Only photons with high energy can excite electrons from the valence band to the conduction band and increase in conductance. Photons with a smaller energy do not have adequate energy to excite electrons from the valence band to the conduction band, thus contributing slightly to the photocurrent.

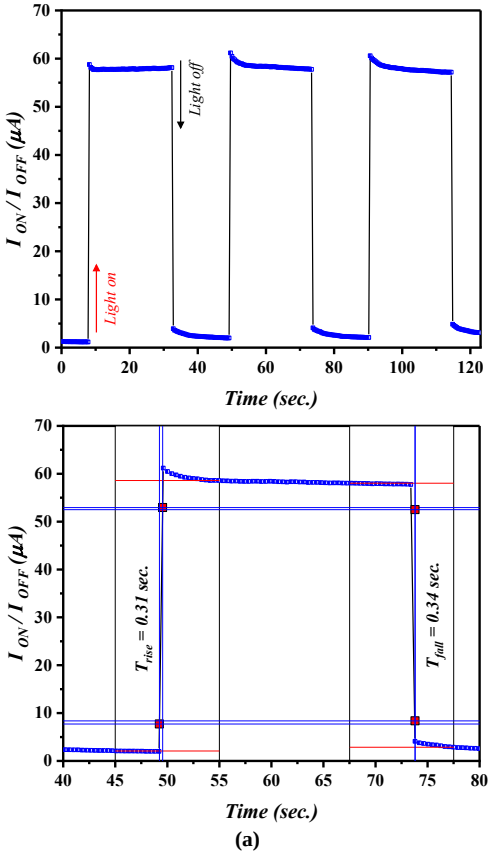

(a)

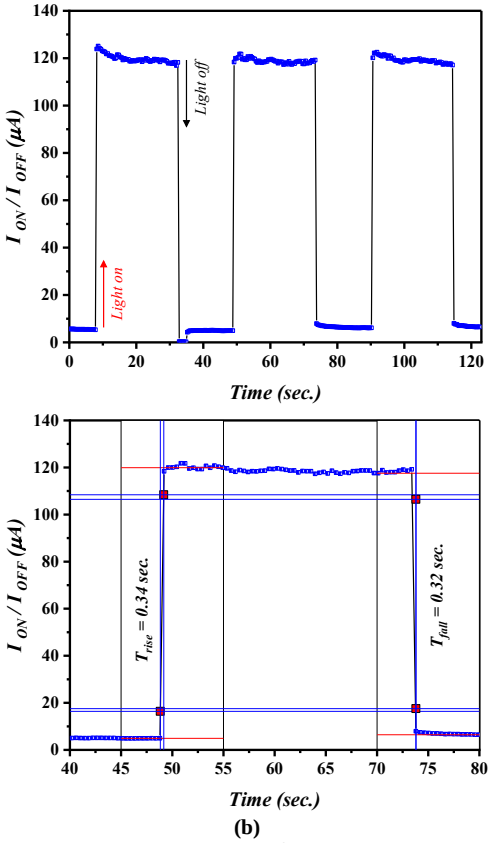

(b)

Fig. (6) Switching behavior of ZnTe/Si photodetectors fabricated at different number of laser pulses (a) 700 pulses and (b) 900 pulses, with response/recovery time

The slight increase in responsivity via long wavelength side is possibly due to the increase in the efficiency of the detector in separating the pairs (electron-holes) generated [26]. The figure shows an increase in the spectral response of the detector from 15.706 µA/mW to 35.758 µA/mW with an increase in the number of laser pulses from 700 to 900. This increase may be due to the decreased resistance, increased photocurrent and the decreased the density of states that act as recombination centres concentrated on two sides of the interface.

Due to the importance of the specific detectivity parameter in detectors, the specific detectivity parameter (D*) was calculated using the following equation [24,25]:

$$D^* = \frac{R_\lambda(A)^{\frac{1}{2}}}{\sqrt{2e\, I_d}}$$

where A is an area of the detector, I_d is the dark current and e is the charge of the electron

Figure (8) shows the specific detectivity of a ZnTe/Si detector fabricated at different numbers of laser pulses. The specific detectivity profile demonstrated similar trend to that of spectral response of the fabricated photodetector. When the number of laser pulses increases from 700 to 900, the detectivity value increases from 7.92×10^{17} Jones to 8.54×10^{17} Jones. The highest detectivity value is at the wavelength of 460 nm. This increase in the detectivity value results from a decrease in the concentration of

 © ALL RIGHTS RESERVED

crystalline defects in the deposited film, which leads to an increase in the value of the spectral response and a decrease in the noise current, and consequently, an increase in the detectivity value of the fabricated detector. The high detectivity of the detector indicates its ability to detect low-energy signals [27].

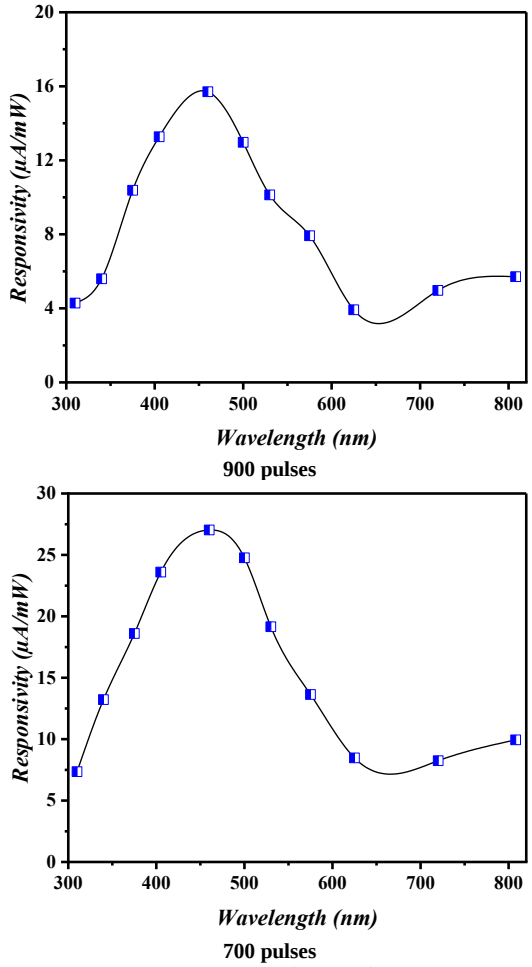

Fig. (7) Photo-responsivity of the fabricated ZnTe/Si photodetectors at 180 mJ and different number of laser pulses

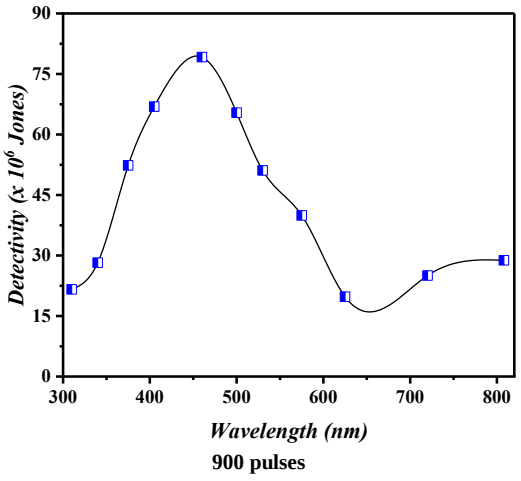

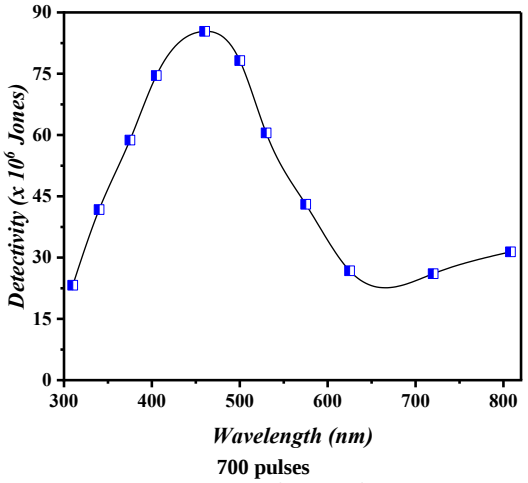

Fig. (8) Photo-detectivity of the fabricated ZnTe/Si photodetectors at 180 mJ and different number of laser pulses

Figure (9) shows the quantum efficiency curve as a function of wavelength for the ZnTe/Si detector, where the quantum efficiency is calculated using the relationship EQE = $\frac{1240\,R_\lambda}{\lambda(nm)}$ [24, 25]. The highest value of the quantum efficiency of the detector that is fabricated at 700 pulses is equal to 42.338% at the wavelength of 460 nm, and this corresponds to the spectral response values of this detector. When the number of laser pulses increases to 900, the quantum efficiency of the detector increases to 72.857% due to the reduction of structural defects, which leads to improving the electrical properties of the detector. Thus, the value of the spectral response increases, which leads to an increase in the quantum efficiency of the detector

4. Conclusion

The effect of the number of laser pulses on the morphological, optical and electrical properties of ZnTe nanostructures was examined and analysed. The XRD data confirmed the growth of the crystalline cubic structure ZnTe. As laser pulses increased, the energy gap decreased from 2.7 eV to 2.62 eV for ZnTe film. FE-SEM revealed the particle size and concentration increased when the number of laser pulses increased. The highest responsivity of the photodetector prepared at 900 pulses was 35.758 μA/mW. The best figures of merit, namely, specific detectivity and quantum efficiency of the photodetector, were 8.54×10^{17} Jones and 72.857%, respectively, which were obtained for a photodetector fabricated at 900 pulses. The photodynamical on/off was demonstrated, and the response and decay times were 0.34 and 0.32 s, respectively. The results revealed that the photodetectors have a typical response/decay time and a good response in the visible region, which is suitable for optical applications.

 © ALL RIGHTS RESERVED

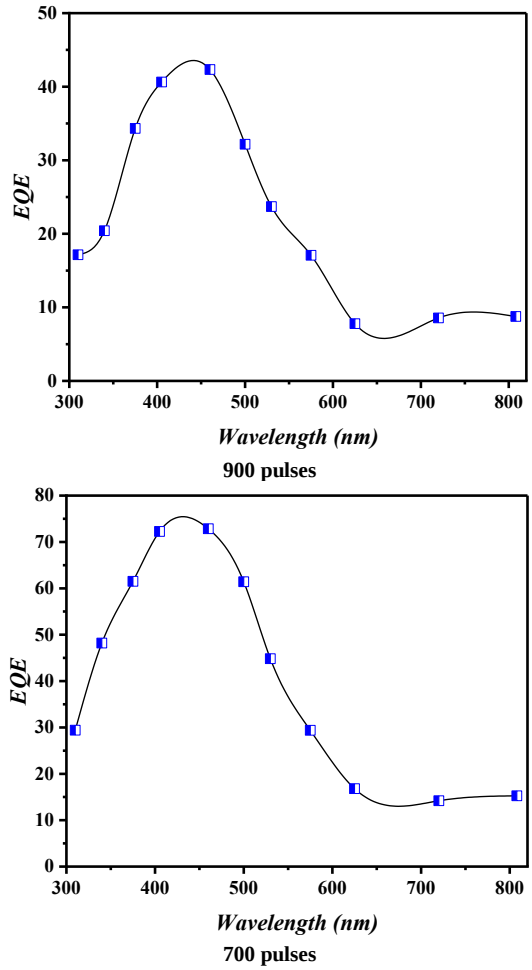

Fig. (9) External quantum efficiency of the fabricated ZnTe/Si photodetectors at 180 mJ and different number of laser pulses

References

[1] H.J. Song et al., "High-performance copper oxide visible-light photodetector via grain-structure model", *Sci. Rep.*, 9(1) (2019) 7334.

[2] V. Adepu et al., "High-performance visible light photodetector based on 1D SnO_2 nanofibers with a $Ti_3C_2T_x$ (MXene) electron transport layer", *ACS Appl. Nano Mater*., 5(5) (2022) 6852–66863.

[3] S. Ma et al., "Discovery of a novel visible-light-active photodetector based on bismuth ferrite: constructing and optimizing the Cr-doped-$BiFeO_3$/NiO thin film heterostructure", *Mater. Today Chem.*, 27 (2023) 101309.

[4] D.-H. Han, S.-J. Choi and S.-M. Park, "Electrochemical preparation of zinc telluride films on gold electrodes", *J. Electrochem. Soc.*, 150(5) (2003) 342-346.

[5] L. Bao et al., "p-type ZnTe:Ga nanowires: controlled doping and optoelectronic device application", *RSC Adv.*, 5 (2015) 13324-13330.

[6] M.S. Hossain, R. Islam and K.A. Khan, "Structural Elemental compositions and Optical properties of ZnTeV", *Thin Films Chalcogen. Lett.*, 7(1) (2010) 21- 29.

[7] D. O'Dell, J.K. Furdyna and X. Liu, "MBE Growth and Characterization of ZnTe and Nitrogen-doped ZnTe on GaAs (100) Substrates", PhD thesis, University of Notre Dame (2010).

[8] B.K.H. AlMaiyaly, B.H. Hussein and A.H. Shaban, "Fabrication and characterization study of ZnTe/n-Si heterojunction solar cell application", *J. Phys.: Conf. Ser.*, 1003 (2018) 012084.

[9] H.Y. Chao et al., "Growth and characterization of type II-ZnO/ZnTe core-shell nanowire arrays for solar cell applications", *Superlat. Microst.*, 47(1) (2010) 160-164.

[10] J. Loferski, *Solid-State Electron.*, 30(11) (1987) 1205.

[11] A.N.S. Al-Shadeedi, "Electronic Properties of a-Ge/c-Si Heterojunction", PhD thesis, University of Baghdad (2009).

[12] T. Ohshima et al., *Surf. Coat. Technol.*, 517 (2003) 169-170.

[13] H. Kressel, **"Semiconductor Lasers and Herterojunction LEDs",** Academic Press (NY, 1977).

[14] G.K. Rao, K.V. Bangera and G. Shivakumar, "Studies on the photoconductivity of vacuum deposited ZnTe thin films", *Mater. Res. Bull.*, 45(10) (2010) 1357-1360.

[15]A.S. Ba-Sabiah and M.A. Seyam, "Some Optical Properties of (ZnTe) Thin Films Prepared by Thermal Evaporation Technique on a Glass Substrate", *Hadhramout Univ. J. Nat. Appl. Sci.*, 14(1) (2017).

[16]A. Ibrahim et al., "Structural and electrical properties of evaporated ZnTe thin films", *Vacuum*, 75(3) (2004) 189-194.

[17] T.M. Amelia, "The synthesis and characterization of the ZnO nanoparticles", MSc thesis, University of the Free State (2011).

[18] D. Manica et al., "Thickness Effect on Some Physical Properties of RF Sputtered ZnTe Thin Films for Potential Photovoltaic Applications", *Nanomaterials*, 11(9) (2021) 2286.

[19] S.A. Maki and H.K. Hassun, "Effect of Aluminum on Characterization of ZnTe/n-Si Heterojunction Photodetector", *J. Phys.: Conf. Ser.*, 1003 (2018) 012085.

[20] S.M. Sze, **"Physics of Semiconductor Devices"**, 3rd ed., John Wiley & Sons (Canada, 2007).

[21] D.A. Neamen, **"Semiconductor Physics and Devices"**, 3rd ed., McGraw-Hill (USA, 2003).

[22] M.Burgelman, P.Nollet and S.Degrave, *Appl. Phys. A*, 69(149) (1999) 423-434.

[23] B.L. Sharma and R.K. Purohit, **"Semiconductor Heterojunctions"**, 1st ed., Pergamon Press (NY, 1974).

[24] Q. Zafar et al., "Organic-inorganic hybrid nanocomposite for enhanced photo-sensing", *J. Nanoparticles Res.*, 17 (2015) 372.

[25] H. K. Hassun, "Study of Photodetector Properties ZnTe:Al/Si prepared by Thermal Evaporation", University of Baghdad (2017).

[26] P. Enghag, **"Encyclopedia of the Elements, Technical Data - History - Processing and Applications"**, Wiley-VCH Press (2004).

[27] Z. Fan et al., "Photoluminescence and polarized photodetection of single ZnO nanowires", *Appl. Phys. Lett.*, 85(25) (2004) 6128-1-6128-3.

 © ALL RIGHTS RESERVED